A MULTIPLE WORKING MODE APPROACH TO CONTROL SPACE MANIPULATOR INTERACTION WITH UNKNOWN TARGETS

Taras Pankov[1], Rabindra Gangapersaud[1], Guangjun Liu[1]

[1] *Department of Aerospace Engineering, Ryerson University, Toronto, Canada, E-mail: gjliu@ryerson.ca*

ABSTRACT

Building upon the multiple working mode robot control approach, we propose to improve the stability and real-time performance of a robotic arm on a servicer satellite performing a capture of, or an interaction task with an unknown target. By switching on-line the working mode of a chosen set of joints to operate in passive mode, passive-like compliance is enabled in the system [1] without the disadvantages associated with free and disconnected drivetrain joints. This work presents two criteria for selection of joints in a serial manipulator for passive mode operation; one criterion considers the torque saturation of the attitude control system, and another criterion is based on the perceived end-effector inertia. The dynamics of the system are formulated with joints working in passive mode, and the effects of the criteria-based working mode selection are investigated with simulations.

1. INTRODUCTION

It is the aim of this work to address in part the challenge of real-time control of a free floating robot manipulator performing a capture of, or an interaction task with an unknown target. The capture process is often decomposed into distinct phases of "approach," "impact," and "stabilization" [2]. The "impact" is the result of rigidization of some degrees of freedom between the manipulator and the target, and can cause high interaction forces when kinematic and dynamic parameters of the target are uncertain. Likewise, during "stabilization", parameter uncertainty can cause disturbance of base attitude and path deviation.

Control of free floating robot manipulator interacting with an unknown target is challenging for several reasons; accurate modelling of the servicer and target system dynamics is not feasible, and the interaction force is difficult to control in practice – even more so in the space environment [3]. In the absence of interaction force measurement, modelling errors could result in interaction forces that exceed the disturbance rejection capabilities of the free-floating servicer satellite attitude control system [4].

For humans, interaction with unknown objects is often a dynamic process, even when our joints are highly compliant (nearly passive) in gait control [5]. Additionally, humans use body inertia to aid in opening of a heavy door, or steering of a heavy cart. In this work, we use passive working mode joints to take the first step towards development of a methodology to utilize the natural robot inertia reducing the torque transmitted to the base from the manipulator following an external disturbance on the end-effector. This approach creates partial reactionless motion of the manipulator without model-based reaction null space motion [6]. With the proposed approach, the generalized coordinates of the system are partitioned such that a set of active joints are position controlled, while the remaining set of passive joints reduces disturbance forces to the base by utilizing inertia coupling between passive joints and the base. Through the use of multiple working mode joints operating in passive mode, we avoid the challenges of model-based control [7], while improving real-time behavior and stability of the system.

Known approaches to control of robotic manipulators with passive joints focus primarily on applications involving constrained interaction tasks such as assembly tasks, or interaction with mechanisms in unstructured environments [8],[9],[10]. There are clear advantages to robotic interaction tasks where the manipulator exhibits passive compliance. For example, interaction forces are reduced in grasping [11] while controllability of the system is not degraded.

Several authors presented controllability analyses of second order non-holonomic systems such as underactuated robotic manipulators and unconstrained motion platforms [12],[13],[14]. When certain controllability conditions are satisfied, such as cyclicity of the passive coordinates [15], the system states are accessible, but there may not exist a smooth controller that converges the states [12].

Some authors have considered the use of passive joints with brakes, such that actuated joints are used to converge the states of the passive joints via dynamic coupling between the joints, and after brakes are engaged to lock the passive joints, actuated joints converge their own states [16]. This two-step approach eliminates in part the controllability issues with second order non-holonomic systems. Another approach considers joints that can disconnect the drivetrain and behave as free joints [17]. Both of these approaches can use the passive "mode" when needed, and fully actuated "modes" when stabilization of manipulator states is needed; however, specialized hardware is required, and a recovery process is needed prior to returning to active control.

Extensive literature exists on force transmission capabilities of underactuated and constrained systems [18],[19]. However, the focus is often on static configuration stability and distribution of constraint forces. Conversely, the dynamics of underactuated systems are of interest in impact analysis. We combine

ideas from both approaches by considering two related problems in *disturbance rejection* from a persistent, time-varying disturbance. The first considers the transmission of force from the point of interaction to the reaction system on the servicer base. The second considers the perceived inertia at the interaction point due to a specific selection of passive joints. The proposed approach promises to improve real-time performance and stability of interaction tasks for free-floating manipulators.

This paper is organized as follows: Section 2 presents the dynamic model, the feedback linearization control with passive joints, the multiple working mode alternative, and the model of the interaction task. The passive joint selection criteria are presented in Section 3, which encompass the primary contributions of this work. Section 4 presents the simulation results, and the directions for future work are outlined in Section 5.

2. METHODOLOGY

2.1 Dynamic Model

The configuration of a free-floating serial manipulator can be described by a set of generalized variables contained in $\boldsymbol{q} \in \mathbb{R}^{m+b=n}$, where m and b are the degrees of freedom (DOF) of the serial manipulator and servicer pose (base) respectively. The manipulator consists of m serial links with $a + p = m$ active and passive joints, and the pose of the base is controlled by r independent reaction inputs such as reaction wheels and thrusters. The relative dimensionality of each term in shown in Fig.1. For convenience, we assume that the pose representation matches the dimensionality of the reaction inputs such; $b = r$. The relationship between the manipulator generalized coordinates, $\boldsymbol{q}$, and task-space coordinates, $\boldsymbol{x} \in \mathbb{R}^e$ is specified by the kinematic relations, $\boldsymbol{\psi}(\boldsymbol{q})\colon \mathbb{R}^n \to \mathbb{R}^e$; $\boldsymbol{\psi}(\boldsymbol{q}) = \boldsymbol{x}$.

Dynamics of the multibody system can be expressed as a system of second order ordinary differential equations, which follow from the Lagrange formulation, and in standard form can be expressed as

$$\boldsymbol{M}(\boldsymbol{q})\ddot{\boldsymbol{q}} + \boldsymbol{h}(\dot{\boldsymbol{q}}, \boldsymbol{q}) = \boldsymbol{\tau} + \boldsymbol{\mathcal{J}}^T\boldsymbol{f} \tag{1}$$

where $\boldsymbol{M} \in \mathbb{R}^{n\times n}$ is the system inertia matrix, $\boldsymbol{h} \in \mathbb{R}^n$ is the vector of the non-linear, joint friction, and gravity forces, and $\boldsymbol{\tau} \in \mathbb{R}^n$ is the vector of generalized actuator forces, $\boldsymbol{\mathcal{J}} \in \mathbb{R}^{e\times n}$ is the base and manipulator Jacobian, $\partial\boldsymbol{\psi}/\partial\boldsymbol{q}$, and $\boldsymbol{f} \in \mathbb{R}^e$ is the interaction force. Given a partitioning of the generalized coordinates into servicer pose and manipulator coordinates, $\boldsymbol{q} = [\boldsymbol{q}_b^T, \boldsymbol{q}_m^T]^T$, one can express the dynamics in (1) as

$$\boldsymbol{M}_b\ddot{\boldsymbol{q}}_b + \boldsymbol{M}_{bm}\ddot{\boldsymbol{q}}_m + \boldsymbol{h}_b = \boldsymbol{\tau}_b + \boldsymbol{\mathcal{J}}_b^T\boldsymbol{f}, \tag{2}$$

$$\boldsymbol{M}_{bm}^T\ddot{\boldsymbol{q}}_b + \boldsymbol{M}_m\ddot{\boldsymbol{q}}_m + \boldsymbol{h}_m = \boldsymbol{\tau}_m + \boldsymbol{\mathcal{J}}_m^T\boldsymbol{f}, \tag{3}$$

where subscripting with $()_b$, $()_{bm}$ and $()_m$ indicates the block matrix corresponding to the partitioning of $\boldsymbol{q}$ into $[\boldsymbol{q}_b^T, \boldsymbol{q}_m^T]^T$. The inertia coupling between base and manipulator is expressed by the block $\boldsymbol{M}_{bm} \in \mathbb{R}^{b\times m}$. Dependency of each term on $\boldsymbol{q}, \dot{\boldsymbol{q}}$ is omitted for clarity.

Finally, the base dynamics equations, (2), can be reduced by eliminating the linear acceleration components of the base as per [15]; this is usually done due to fuel constraints in thruster-based actuation, and due to the greater importance to control the base attitude than its position. The proposed approach is applicable when $\boldsymbol{q}_b \in \mathbb{R}^3$ contains only the rotation representation of the base.

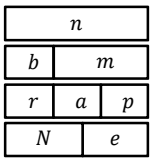

n: generalized coordinates
m: manipulator coordinates
b: base coordinates / r:reaction inputs
a: active joints / p: passive joints
e: end effector task space dimension
N: dimensionality of nullspace w.r.t. task

Figure 1: Relative Dimensionality of System Coordinates.

2.2 Control With Passive Joints

The control torque for base and manipulator subsystems which will achieve tracking of a desired task, specified by $\boldsymbol{q}^* = [\boldsymbol{q}_b^{*T}, \boldsymbol{q}_m^{*T}]^T$ and its derivatives, is from computed torque as

$$\boldsymbol{\tau}_b = \boldsymbol{M}_b\ddot{\boldsymbol{q}}_b^* + \boldsymbol{M}_{bm}\ddot{\boldsymbol{q}}_m^* + \boldsymbol{h}_b - \boldsymbol{\mathcal{J}}_b^T\boldsymbol{f}, \tag{4}$$

$$\boldsymbol{\tau}_m = \boldsymbol{S}_a(\boldsymbol{M}_{bm}^T\ddot{\boldsymbol{q}}_b^* + \boldsymbol{M}_m\ddot{\boldsymbol{q}}_m^* + \boldsymbol{h}_m - \boldsymbol{\mathcal{J}}_m^T\boldsymbol{f}). \tag{5}$$

The diagonal elements of the input matrix $\boldsymbol{S}_a$ set the passive joint control torque to zero. Substituting the control torque (4) into the base dynamics (2), and neglecting modelling errors and error correction terms, the base dynamics reduce to

$$\boldsymbol{M}_b(\ddot{\boldsymbol{q}}_b - \ddot{\boldsymbol{q}}_b^*) + \boldsymbol{M}_{bm}(\ddot{\boldsymbol{q}}_m - \ddot{\boldsymbol{q}}_m^*) = \boldsymbol{0}. \tag{6}$$

Considering a control objective for the manipulator as $\ddot{\boldsymbol{q}}_m^* = \boldsymbol{S}_a\ddot{\boldsymbol{q}}_m^* + \boldsymbol{S}_p\ddot{\boldsymbol{q}}_m$, where $\boldsymbol{S}_p = \boldsymbol{I} - \boldsymbol{S}_a$, the dynamics in (3) with control torque from (5) partition into active and passive sets;

$$\boldsymbol{S}_a\big(\boldsymbol{M}_{bm}^T(\ddot{\boldsymbol{q}}_b - \ddot{\boldsymbol{q}}_b^*) + \boldsymbol{M}_m\boldsymbol{S}_a(\ddot{\boldsymbol{q}}_m - \ddot{\boldsymbol{q}}_m^*)\big) = \boldsymbol{0}, \tag{7}$$

$$\boldsymbol{S}_p(\boldsymbol{M}_{bm}^T\ddot{\boldsymbol{q}}_b + \boldsymbol{M}_m\ddot{\boldsymbol{q}}_m + \boldsymbol{h}_m - \boldsymbol{\mathcal{J}}_m^T\boldsymbol{f}) = \boldsymbol{0}. \tag{8}$$

The combined system modelled by (6)-(8) is satisfied by the solution $\ddot{\boldsymbol{q}}_b = \ddot{\boldsymbol{q}}_b^*$, and $\ddot{\boldsymbol{q}}_m = \boldsymbol{S}_p\ddot{\boldsymbol{q}}_m + \boldsymbol{S}_a\ddot{\boldsymbol{q}}_m^*$; acceleration of the passive joints is in the null space of the task for active joints (although this neglects the possibility that high-level task definition may depend on passive joints). The solution for the joint accelerations is as

$$\ddot{\boldsymbol{q}}_m = \big(\boldsymbol{S}_p\boldsymbol{M}_m\boldsymbol{S}_p\big)^+(\boldsymbol{\mathcal{J}}_m^T\boldsymbol{f} - \boldsymbol{M}_{bm}^T\ddot{\boldsymbol{q}}_b^* - \boldsymbol{h}_m) + \boldsymbol{S}_a\ddot{\boldsymbol{q}}_m^*. \tag{9}$$

2.3 Multiple Working Mode Control

The dynamics expressed by (7) are the result of perfect compensation with a feedback linearizing computed torque. However, it may not be practical to assume that an accurate dynamics model of the servicer system is available. We assume that joint torque estimates are available either through torque sensors at each joint, or through momentum residual error estimates [20]. With known joint torque at the output shaft, a multiple working mode approach is used to achieve the partitioning of dynamics into active and passive sets of variables. With the model considered here, illustrated in Fig. 2, the ideal torque sensor measurement

$\boldsymbol{\tau}_{sensor} = \boldsymbol{\tau}_m$ is available.

The manipulator dynamics in (3) can be separated into link and motor components as follows

$$\boldsymbol{M}_l\ddot{\boldsymbol{q}}_m + \boldsymbol{M}_{bm}^T\ddot{\boldsymbol{q}}_b + \boldsymbol{h}_l = \boldsymbol{\tau}_m + \boldsymbol{\mathcal{J}}_m^T\boldsymbol{f} \quad (10)$$

$$\boldsymbol{M}_s\ddot{\boldsymbol{q}}_m + \boldsymbol{h}_s + \boldsymbol{\tau}_m = \boldsymbol{\Gamma}\boldsymbol{\tau}_s \quad (11)$$

where subscripting with $(\,)_s$ and $(\,)_l$ denotes motor shaft and link dynamics properties respectively, $\boldsymbol{\Gamma} = \mathrm{diag}[\gamma_1 \ldots \gamma_n]$ is the matrix of motor gearing ratios, and $\boldsymbol{\tau}_s \in \mathbb{R}^m$ is the motor torque. As per [1], the dynamics (10) for motor i are

$$\boldsymbol{I}_{mi}\gamma_i\big(\gamma_i\ddot{q}_i + \textstyle\sum_{j=1}^{i-1}\boldsymbol{z}_{mi}^T\boldsymbol{z}_j\ddot{q}_j + \sum_{j=2}^{i-1}\sum_{k=1}^{j-1}\boldsymbol{z}_{mi}^T(\boldsymbol{z}_k\cdot\boldsymbol{z}_j)\dot{q}_k\dot{q}_j\big) + \\ +\gamma_i\tau_{fi} + \tau_{si} = \gamma_i\tau_{mi}. \quad (12)$$

For joint i, $\boldsymbol{I}_m$ is the joint motor inertia, $\boldsymbol{z}_m$ and $\boldsymbol{z}$ are the rotor axis and joint axis direction vectors respectively. The friction term parameters f_{ki}, b_i, $f_{si}, f_{\tau i}$, representing the Coulomb, viscous, and Stribeck components respectively, is modelled by

$$\tau_{fi}(q_i, \dot{q}_i) = [f_{ki} + f_{si}\exp(-f_{\tau i}\dot{q}_i^2)]\mathrm{sgn}(\dot{q}_i) + b_i\dot{q}_i. \quad (13)$$

Using estimates of the motor dynamics properties ($\hat{}$), and the measured motor shaft torque, $\boldsymbol{\tau}_s$, the dynamics compensation equation for (11) is

$$\boldsymbol{\Gamma}\boldsymbol{\tau}_s = \boldsymbol{\tau}_s^a = \hat{\boldsymbol{\tau}}_m + \hat{\boldsymbol{h}}_s + \hat{\boldsymbol{M}}_s\ddot{\boldsymbol{q}}_m^* + \boldsymbol{K}_d\dot{\boldsymbol{e}}_m + \boldsymbol{K}_p\boldsymbol{e}_m \quad (14)$$

$\ddot{\boldsymbol{q}}^*$ is the desired acceleration obtained from higher-level task specification, $\boldsymbol{K}_d$ and $\boldsymbol{K}_p$ are positive definite control gain matrices, and $\boldsymbol{e}_m = \boldsymbol{q}_m^* - \boldsymbol{q}_m$ is the joint position error. The resulting dynamics in (11) reduce to the error dynamics;

$$\ddot{\boldsymbol{e}}_m + \boldsymbol{M}_m^{-1}\boldsymbol{K}_d\dot{\boldsymbol{e}}_m + \boldsymbol{M}_m^{-1}\boldsymbol{K}_p\boldsymbol{e}_m = 0. \quad (15)$$

The controller defined by (14) is termed as *active* mode control in the multiple working mode control framework; it is able to compensate for link dynamics and external forces via the torque sensor measurement. Alternatively, *passive* mode control is obtained by setting $\boldsymbol{q}_m^* \equiv \boldsymbol{q}_m$, $\dot{\boldsymbol{q}}_m^* \equiv \dot{\boldsymbol{q}}_m$, and $\ddot{\boldsymbol{q}}_m^* \equiv \boldsymbol{0}$, i.e. $\boldsymbol{e} \equiv \boldsymbol{0}$;

$$\boldsymbol{\Gamma}\boldsymbol{\tau}_s = \boldsymbol{\tau}_s^p = \check{\boldsymbol{h}}_s, \quad (16)$$

where $\check{\boldsymbol{h}}_s$ compensates only the static component of friction from (13). The dynamics resulting from this controller are as

$$\ddot{\boldsymbol{q}}_m + \boldsymbol{M}_m^{-1}\big(\hat{\boldsymbol{h}}_s - \check{\boldsymbol{h}}_s\big) + \boldsymbol{\tau}_m = \boldsymbol{0}. \quad (17)$$

Temporarily modelling $\boldsymbol{\tau}_m$ as the torque in a stiff motor shaft with $\boldsymbol{K}_s \gg \boldsymbol{K}_p$ and $\boldsymbol{q}_l$ as the link position; $\boldsymbol{\tau}_m = \boldsymbol{K}_s(\boldsymbol{q}_l - \boldsymbol{q}_m) = \boldsymbol{K}_s\boldsymbol{e}_m$, it can be shown that the dynamics of (17) reduce to

$$\ddot{\boldsymbol{e}}_m + \boldsymbol{M}_m^{-1}(\hat{\boldsymbol{h}}_s - \check{\boldsymbol{h}}_s)\dot{\boldsymbol{e}}_m + \boldsymbol{M}_m^{-1}\boldsymbol{K}_s\boldsymbol{e}_m = \boldsymbol{0}. \quad (18)$$

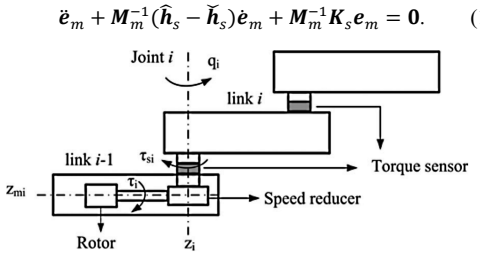

Figure 2: Schematic for the motor dynamics formulation.

Clearly (18) tracks the link position, and that the time constant for this system is much smaller than that of (15); $\boldsymbol{\tau}_m \to \boldsymbol{0}$ as $t \to \infty$.

We can unify the active and passive control modes by employing the selection matrix from (5);

$$\boldsymbol{\Gamma}\boldsymbol{\tau}_m = \boldsymbol{S}_a\boldsymbol{\tau}_s^a + \boldsymbol{S}_p\boldsymbol{\tau}_s^p. \quad (19)$$

For clarity, the presence of modelling errors and error compensation is neglected, and the combined system dynamics from (10,11) is as

$$\boldsymbol{0} = \boldsymbol{S}_a\ddot{\boldsymbol{e}}_m + \\ \boldsymbol{S}_p(\boldsymbol{M}_{bm}^T\ddot{\boldsymbol{q}}_b + (\boldsymbol{M}_s + \boldsymbol{M}_l)\ddot{\boldsymbol{q}}_m + (\boldsymbol{h}_s + \boldsymbol{h}_l) - \boldsymbol{\mathcal{J}}_m^T\boldsymbol{f}), \quad (20)$$

which is equivalent to the partitioning in (7,8). However, the control laws used here do not require an accurate dynamics model. Furthermore, the joints in passive mode do not require state feedback, eliminating a source of instability in interaction tasks.

2.4 Task Description

Maintaining attitude for space manipulators is often mission-critical. An external disturbance such as a continuous interaction with a target, or an impulse interaction such as a collision or rigidization event injects linear and angular momentum into the system. Through the control law in (4), this disturbance is immediately and entirely compensated by the base attitude control system, such as a set of reaction wheels. To model the disturbance, we consider a robotic or extravehicular activity where the servicer/manipulator system maintains position of the end effector and is subjected to a constant, bounded load; $\boldsymbol{f} \in \mathbb{R}^e$. Joints are in active working mode maintaining position via the control input in (14).

The reaction system is subject to input saturation, $\boldsymbol{\tau}_b(i) \le \boldsymbol{\tau}_b^{sat}(i), \forall i = 1{:}\,b$. To ensure that this input saturation is not exceeded, the manipulator motion is used to partially offset the external disturbance and reduce the force transfer to the attitude control system; usually this involves computed torque methods with joints working in active mode. With our approach, some joints are switched to passive working mode so that the acceleration of passive joints partially absorbs excess momentum transfer to the servicer reaction control system until the disturbance is removed.

3. MODE SELECTION

3.1 Reduction of Disturbance on Servicer

Expressing (2) for control input $\boldsymbol{\tau}_b$ and substituting the solution for $\ddot{\boldsymbol{q}}_m$ from (7,8), one obtains

$$\boldsymbol{\tau}_b = \boldsymbol{M}_b\ddot{\boldsymbol{q}}_b^* + \boldsymbol{M}_{bm}\big(\boldsymbol{S}_a\ddot{\boldsymbol{q}}_m^* + \boldsymbol{S}_p\ddot{\boldsymbol{q}}_m\big) + \boldsymbol{h}_b - \boldsymbol{\mathcal{J}}_b^T\boldsymbol{f}, \quad (21)$$

with $\boldsymbol{S}_p\ddot{\boldsymbol{q}}_m$ being the first term on the r.h.s of (9). For passive joints initially at rest, and by setting the control variables $\ddot{\boldsymbol{q}}_b^* = \boldsymbol{0}$, $\boldsymbol{S}_a\ddot{\boldsymbol{q}}_m^* = \boldsymbol{0}$, the relationship simplifies into a mapping from the disturbance force onto the servicer base generalized forces via the dynamic or generalized Jacobian;

$$\boldsymbol{\tau}_b = \Big(\boldsymbol{M}_{bm}\big(\boldsymbol{S}_p\boldsymbol{M}_m\boldsymbol{S}_p\big)^+\boldsymbol{\mathcal{J}}_m^T - \boldsymbol{\mathcal{J}}_b^T\Big)\boldsymbol{f}. \quad (22)$$

Notice that $\boldsymbol{S}_p$ selects the accelerations of passive joints and maps their effect onto the base via the inertial coupling $\boldsymbol{M}_{bm}$.

Either of these expressions can be used to select a set of passive joints that improve or optimize a performance metric on $\boldsymbol{\tau}_b$ such as

$$\boldsymbol{S}_p(i^*, i^*) = 1,\ i^* = \underset{i}{\operatorname{argmin}}(\max(\boldsymbol{\tau}_b^{sat})^{-1}\boldsymbol{\tau}_b), \quad (23)$$

which selects a passive joint that obtains the min-max reaction onto the base, normalized by the actuator saturation force, $\boldsymbol{\tau}_b^{sat}$.

For a known direction of disturbance force, the structure of (22) allows for a more direct method for selection of passive joints than is possible via (23);

$$\boldsymbol{\tau}_b = \left(\boldsymbol{M}_{bm}\boldsymbol{S}_p\left(\operatorname{diag}(\boldsymbol{M}_m)\right)^{-1}\boldsymbol{S}_p\boldsymbol{\mathcal{J}}_m^T\boldsymbol{f} - \boldsymbol{\mathcal{J}}_b^T\boldsymbol{f}\right). \quad (24)$$

With $\boldsymbol{k}_{bm}^i$ representing column i of $\boldsymbol{M}_{bm}$, M_m^i the i-th diagonal entry of $\boldsymbol{M}_{\boldsymbol{m}}$, f_m^i the i-th element of $\boldsymbol{\mathcal{J}}_m^T\boldsymbol{f}$, and $\boldsymbol{f}_b$ the product $\boldsymbol{\mathcal{J}}_b^T\boldsymbol{f}$, reaction onto the base from setting the i-th joint to passive mode is

$$\boldsymbol{\tau}_b^i = \boldsymbol{k}_{bm}^i {M_m^i}^{-1} f_m^i - \boldsymbol{f}_b. \quad (25)$$

The criteria according to (23) is therefore

$$i^* = \underset{i}{\operatorname{argmin}}\left(\max\left(\left|\boldsymbol{k}_{bm}^i {M_m^i}^{-1} f_m^i - \boldsymbol{f}_b\right|\right)\right). \quad (26)$$

When considering the saturation force, $\boldsymbol{\tau}_b^{sat}$;

$$i^* = \underset{i}{\operatorname{argmin}}\left(\max\left(\left|\boldsymbol{k}_{bm}^i {M_m^i}^{-1} f_m^i - \boldsymbol{f}_b\right| - \boldsymbol{\tau}_b^{sat}\right)\right). \quad (27)$$

3.2 Shaping of Perceived Task-Space Inertia

In defining the task for active joints as a desired trajectory in joint space, $\ddot{\boldsymbol{q}}_m^*$, we did not consider the effect of the passive joint on the ability of the manipulator to follow a trajectory in operational space. One would desire to select a passive joint that results in the least deformation of the task space trajectory, while reducing the reaction forces at the servicer base below saturation limits. For the simplified task of maintaining a constant setpoint, $\dot{\boldsymbol{q}}_m^* = \boldsymbol{0}$, we can define another selection criteria that reduces task-space acceleration due to the uncompensated component of the disturbance force, $\boldsymbol{f}$. Substituting the manipulator acceleration solution from (9), the kinematic relationship, $\boldsymbol{\mathcal{J}}_b\dot{\boldsymbol{q}}_b + \boldsymbol{\mathcal{J}}_m\dot{\boldsymbol{q}}_m = \dot{\boldsymbol{x}}$, can be expressed as

$$\ddot{\boldsymbol{x}} = \boldsymbol{\mathcal{J}}_b\ddot{\boldsymbol{q}}_b^* + \dot{\boldsymbol{\mathcal{J}}}_b\dot{\boldsymbol{q}}_b + \dot{\boldsymbol{\mathcal{J}}}_m\dot{\boldsymbol{q}}_m + \boldsymbol{\mathcal{J}}_m\left(\left(\boldsymbol{S}_p\boldsymbol{M}_m\boldsymbol{S}_p\right)^+(\boldsymbol{M}_{bm}^T\ddot{\boldsymbol{q}}_b^* + \boldsymbol{h}_m - \boldsymbol{\mathcal{J}}_m^T\boldsymbol{f}) + \boldsymbol{S}_a\ddot{\boldsymbol{q}}_m^*\right), \quad (28)$$

and for a system at rest with constant setpoint,

$$\ddot{\boldsymbol{x}} = \boldsymbol{\mathcal{J}}_m\left(\boldsymbol{S}_p\boldsymbol{M}_m\boldsymbol{S}_p\right)^+\boldsymbol{\mathcal{J}}_m^T\boldsymbol{f}. \quad (29)$$

This result is similar to the dynamic Jacobian used in impact analysis for momentum distribution [2][18][19]. Here, the use of perfect tracking in active joints controller results in an apparently infinite inertia along directions of active joints. By switching some joints to passive working mode, only the inertia of the passive joint, M_m^i, is mapped onto the end effector. Generally, a joint furthest away from the end effector working in passive working mode will result in the greatest projected inertia in operational space and thus meet the criteria for reduction of task deformation. For selection of a single passive joint, the criteria can be specified as

$$\boldsymbol{S}_p(i^*, i^*) = 1,\quad i^* = \underset{i}{\operatorname{argmin}}\left(\max\left(\boldsymbol{k}_{\mathcal{J}_m}^i {M_m^i}^{-1} f_m^i - \boldsymbol{f}_b\right)\right), \quad (30)$$

where $\boldsymbol{k}_{\mathcal{J}_m}^i$ is a column of $\boldsymbol{\mathcal{J}}_m$.

4. SIMULATION

In this section the effectiveness of the passive joint selection for reduction of base reaction forces is demonstrated. The reaction wheels at the base compensate fully for the torque disturbance due to external forces as well as motion of the manipulator arm as per the control law in (2), although any controller capable of maintaining attitude is acceptable. Additionally, the dynamics of the base and manipulator have been reformulated as per [6] to account for lack of actuation in base translation.

4.1 Criteria Evaluation

In the planar case with a 3DOF manipulator, shown in Fig. 3 with parameters in Table 1, the reaction torque on the single reaction wheel τ_b is computed for configurations between $\boldsymbol{q}_i$ (as shown in Fig. 3) and $\boldsymbol{q}_f$ (stretched out) with one of the three joints working in passive mode. The transition from $\boldsymbol{q}_i$ to $\boldsymbol{q}_f$ does not represent the motion resulting from application of force or control; instead, we only evaluate the reaction forces at the particular configuration and selection of passive joints as per the criteria in (26). We also consider a baseline case with all joints in active mode. Unit forces along the two translation directions X and Y in the inertial frame, Σ_I, and a unit torque along the rotation direction Z are applied to the end effector. See Fig. 3 for schematic and axes directions.

From Fig. 4, when force is applied along X direction, selection of the first joint to operate in passive mode results in negligible reduction of reaction torque. However, when a force along the Y direction is applied, any of the three joints can operate in passive mode to reduce the reaction onto the servicer.

Lastly, the selection is non-intuitive with application of torque along Z direction; selecting joint 1 for operation

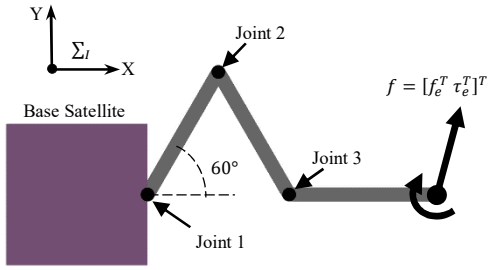

Figure 3: Planar space manipulator configuration. Link and servicer base properties are detailed in Table 1.

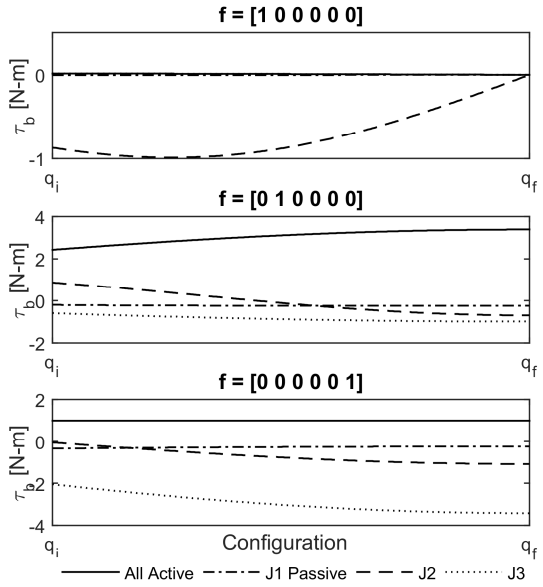

Figure 4: Reaction torque required to maintain attitude under different selected passive joints.

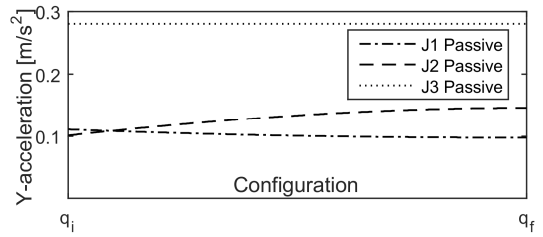

Figure 5: Measure of task deformation.

in passive mode reduces the reaction torque significantly, but joint 3 in passive mode magnifies the reaction torque. The non-intuitive nature of the selection is in part due to the complex inertial coupling resulting from elimination of the translational dynamics of the servicer base.

From Fig. 5, for the case of force applied along Y direction, the end effector acceleration along the same direction is shown. The selection criteria from (26) is in agreement with (21) for only a subset of the configurations between $\boldsymbol{q}_i$ and $\boldsymbol{q}_f$.

4.2 Application in Simulation

A 7DOF spacial manipulator on a base controlled by reaction wheels is shown in Fig. 6, with parameters in Table 2, the dynamics are simulated for the application of a sinusoidal force at the end effector. The applied force switches between unit vectors on X,Y,Z force, followed by unit vectors on X,Y,Z torque every 1 second. The applied force and torque are defined with respect to the inertial frame in Fig. 6, Σ_I.

For all joints working in active mode, disturbance is fully rejected by the manipulator, but torques on the reaction wheels are generally greater than in the case where one of the seven joints operates in passive mode. Figure 7 demonstrates this behavior

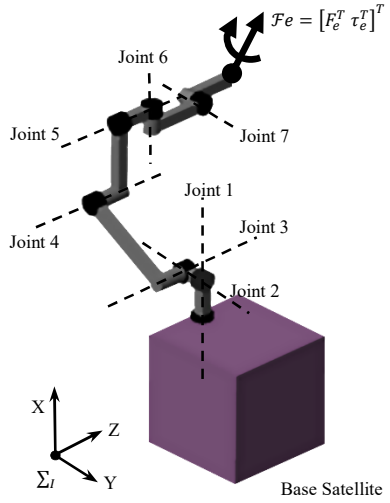

Figure 6: 7DOF space manipulator configuration. Link and servicer base parameters are detailed in Table 2, and Denavit-Hartenberg parameters are as per [21].

To gain a clearer understanding of the resultant reactions, in selecting passive joints, we consider one reaction wheel at a time instead of (21);

$$i^* = \underset{i}{\operatorname{argmin}}\left(\left(\boldsymbol{k}_{bm}^i M_m^{i\,-1} f_m^i - \boldsymbol{f}_b\right)^j\right), \qquad (31)$$

where $(\,)^j$ indicates j-th element of the set. Passive joints are enabled as needed when an external force is applied. In all cases, it is possible to reduce the reaction wheel torque by setting a joint to operate in passive mode. In Fig. 7, the index of the selected passive joint is shown for each segment of the simulation.

In transitioning from passive mode back to active, the accumulated joint position error becomes a step input to the active controller, which results in a large induced reaction to the base until the active controller rejects the accumulated error. To overcome this, one would

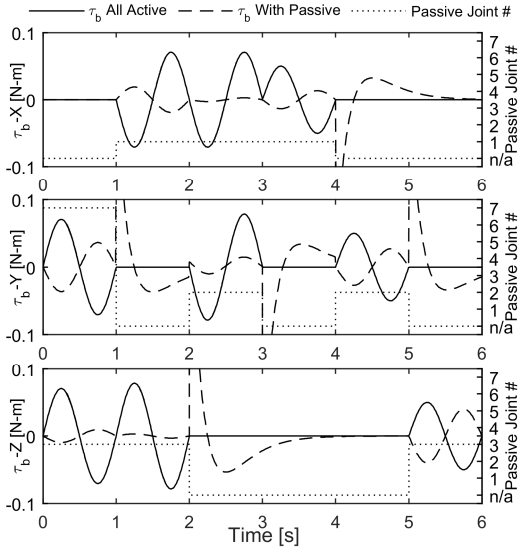

Figure 7: Reaction torque required to maintain attitude.

Table 1: Three DOF Model Parameters.

	Mass (kg)	Izz(kgm^2)	Dimension [m]
Base	500	100	1×1
Link 1	10	1.05	1×0.1
Link 2	10	1.05	1×0.1
Link 3	10	1.05	1×0.1
RW z	1	0.1	Radius=0.5

Table 2: Seven DOF Model Parameters.

	Mass(kg)	Ixx(kgm^2)	Iyy(kgm^2)	Izz(kgm^2)
Base	1000	1200	1200	1200
Link 1	35.01	1.218	0.5132	1.331
Link 2	30	2.10	1.378	2.359
Link 3	22.69	0.102	3.378	3.359
Link 4	21.38	0.4327	2.266	1.911
Link 5	16.75	0.3878	0.3963	0.07271
Link 6	26.17	0.5727	0.5987	0.1288
Link 7	18.07	0.165	0.241	0.135
RW x	1	0.10	0.10	0.10
RW y	1	0.10	0.10	0.10
RW z	1	0.10	0.10	0.10

design a *post-passive* mode which would stabilize the joint without exceeding torque limitations of the base attitude control, and only then return the joint to active mode control. In this work, we are only concerned with passive mode operation.

5. CONCLUSION

The dynamics of the system were developed to incorporate the passive joint selection, and criteria for selection of passive joints were generated based on pertinent metrics in space manipulator tasks. Specifically, we considered the disturbance reaction torques on the servicer base, and task deformation at the end effector.

Future work will examine the controllability implications of a particular selection of passive joints by considering a specific task such as detumbling of an uncooperative target or trajectory control of the manipulator. Additionally, we will work on designing a new joint working mode – post-passive damping mode – to aid in the transition from passive to active mode based on the active controller being utilized.

REFERENCES

[1] G. Liu, X. He, J. Yuan, S. Abdul and A.A. Goldenberg, "Development of modular and reconfigurable robot with multiple working modes," *IEEE Int. Conf. on Robotics and Automat., ICRA*, Pasadena, CA, pp. 3502-07, 2008.

[2] D.N. Nechev and K. Yoshida, "Impact analysis and post-impact control issues of a free floating space robot subject to a force impulse," *IEEE Trans. on Robotics and Automat.,* vol. 15, no. 3, pp. 548-557, 1999.

[3] R. Volpe, "Techniques for collision prevention, impact stability, and force control by space manipulators," in *Teleoperation and Robotics in Space*, Washington, D.C.: AAAI, pp. 175-208, 1994.

[4] T. Oki, S. Abiko, H. Nakanishi, and K. Yoshida, "Time-optimal detumbling maneuver along an arbitrary arm motion during the capture of a target satellite," *IEEE/RSJ Int. Conf. on Intell. Robots and Syst.*, San Francisco, CA, pp. 625-230, 2011.

[5] S. Collins, A. Ruina, R. Tedrake and M. Wisse, "Efficient Bipedal Robots Based on Passive-Dynamic Walkers," *Science*, vol. 307, no. 5712, pp. 1082-85, 2005.

[6] D.N. Nechev and K. Yoshida, "Impact analysis and post-impact control issues of a free floating space robot subject to a force impulse," *IEEE Trans. on Robotics and Automation.*, vol. 15, no. 3, pp. 548-557, 1999.

[7] G. Liu, S. Abdul and A.A. Goldenberg, "Stabilizing Modular and Reconfigurable Robot Joint by Joint Using Torque Sensing," *Robotica,* vol. 26, no. 1, pp. 75-84, 2008

[8] N. McClamroch and D. Wang, "Feedback stabilization and tracking of constrained robots," *IEEE Trans. on Automat. Control*, vol. 33, no. 5, pp. 419-426, 1988.

[9] T. Nef and P. Lum, "Improving backdrivability in geared rehabilitation robots," *Medical & Biological Eng. & Comput.*, vol. 47, no. 4, pp. 441-447, 2009.

[10] T. Pankov and G. Liu, "Multiple Working Mode Approach to Manipulation of Unknown Mechanisms Using a Serial Robot," *Proc. of Int. Conf. on Cyber Tech. in Automat., Control and Intell. Sys., IEEE*, Shenyang, China, pp. 13-18, 2015.

[11] L. Birglen, T. Laliberte and C. Gosselin, "Kinetostatic Analysis of Robotic Fingers," in *Underactuated Robotic Hands*, Germany, Springer, ch. 3, pp. 33–60, 2008.

[12] M. Reyhanoglu, A. van der Schaft, N. McClamroch and I. Kolmanovsky, "Dynamics and control of a class of underactuated Mechanical systems," *IEEE Trans. on Automat. Control*, vol. 44, no. 9, pp. 1663-71, 1999.

[13] W. Blajer and K. Kolodziejczyk, "A case study of inverse dynamics control of manipulators with passive joints," J. of Theoretical and Applied Mech., vol. 52, no. 3, pp. 793-801, 2014.

[14] H. Arai, K. Tanie and S. Tachi, "Dynamic Control of a Manipulator with Passive Joints in Operational Space," *IEEE Trans. on Robotics and Automat., vol. 9, no. 1*, pp. 85-93, 1993.

[15] K. Yoshida and D. Nenchev, "Reaction Null-Space Based Control of Under-Actuated Manipulators," *Proc. Of the Int. Conf. on Intell. Robots and Systems, IEEE"*, Victoria, BC, pp. 1358-1363, 1998.

[16] H. Arai and S. Tachi, "Dynamic Control of a Manipulator with Passive Joints in an Operational Coordinate Space," *Proc. of the Int. Conf. on Robotics and Automat., IEEE,* Sacramento, CA, pp. 1188-94, 1991.

[17] N. Aiguo, M. Satou, T. Kamimura and Y. Hasegawa, "Automatic insertion of a long-pipe by a mobile manipulator with exchangeable active/passive joints," *Int. Conf. on Systems, Man, and Cybernetics, IEEE Vol.1*, Tucson, AZ, pp. 359-364, 2001.

[18] K. Yoshida, "A General Formulation for Under-Actuated Manipulators," *Proc. of the Int. Conf. on Intell. Robots and Sys., IROS'97, IEEE*, Grenoble, pp. 1651-1657, 1997.

[19] Y. Xu, "The Measure of Dynamics Coupling of Space Robot Systems", *Proc. of the Int. Conf. on Robotics and Automat., IEEE*, Atlanta, GA, pp. 615-620, 1993.

[20] A. De Luca, A. Albu-Schaffer, S. Haddadin and G. Hirzinger, "Collision Detection and Safe Reaction with the DLR-III Lightweight Manipulator Arm", *Proc. of the Int. Conf. on Robotics and Systems, IEEE,* Beijing, China, pp.1623-1630, 2006.

[21] T.C. Nguyen-Huynh and I. Sharf, "Adaptive reactionless motion and parameter identification in postcapture of space debris, " *J. of Guidance, Control, and Dyn.*, vol. 36, no. 2, pp. 404-414, 2013.